



The potential of radar-based ensemble forecasts for flash-flood early warning in the southern Swiss Alps

K. Liechti¹, L. Panziera², U. Germann², and M. Zappa¹

¹Swiss Federal Research Institute WSL, Birmensdorf, Switzerland

²MeteoSwiss, Locarno Monti, Switzerland

Correspondence to: K. Liechti (kaethi.liechti@wsl.ch)

Received: 11 January 2013 – Published in Hydrol. Earth Syst. Sci. Discuss.: 25 January 2013

Revised: 26 August 2013 – Accepted: 28 August 2013 – Published: 10 October 2013

Abstract. This study explores the limits of radar-based forecasting for hydrological runoff prediction. Two novel radar-based ensemble forecasting chains for flash-flood early warning are investigated in three catchments in the southern Swiss Alps and set in relation to deterministic discharge forecasts for the same catchments. The first radar-based ensemble forecasting chain is driven by NORA (Nowcasting of Orographic Rainfall by means of Analogues), an analogue-based heuristic nowcasting system to predict orographic rainfall for the following eight hours. The second ensemble forecasting system evaluated is REAL-C2, where the numerical weather prediction COSMO-2 is initialised with 25 different initial conditions derived from a four-day nowcast with the radar ensemble REAL. Additionally, three deterministic forecasting chains were analysed. The performance of these five flash-flood forecasting systems was analysed for 1389 h between June 2007 and December 2010 for which NORA forecasts were issued, due to the presence of orographic forcing.

A clear preference was found for the ensemble approach. Discharge forecasts perform better when forced by NORA and REAL-C2 rather than by deterministic weather radar data. Moreover, it was observed that using an ensemble of initial conditions at the forecast initialisation, as in REAL-C2, significantly improved the forecast skill. These forecasts also perform better than forecasts forced by ensemble rainfall forecasts (NORA) initialised from a single initial condition of the hydrological model. Thus the best results were obtained with the REAL-C2 forecasting chain. However, for regions where REAL cannot be produced, NORA might be an option for forecasting events triggered by orographic precipitation.

1 Introduction

To issue early warnings about flash floods, information about the spatial and temporal distribution of precipitation is crucial. Catchments with steep slopes and shallow soils, which are typical in the Alps, specifically react very quickly to intense rainfall. Forecasting for flash-flood events would thus help to extend the time available to issue warnings and implement safety measures. Producing such forecasts is, however, a very challenging task. A first challenge is to model the physical processes that affect the runoff generation. This involves uncertainties in the model structure and parameterization. Also finding an adequate initial state for the initialisation of a hydrological forecast is not trivial, but important especially for short-term forecasts, as this state can have a significant influence on the model output at the beginning of the simulations (AghaKouchak et al., 2013). Fundel and Zappa (2011) compared ensemble forecasts initialised by states obtained by reference runs of a hydrological model using meteorological observations and meteorological reanalysis (ERA-interim) data. The resulting forecasts showed significantly better skill using initialisations based on meteorological observations especially for the first forecast days. In an experimental framework Zappa et al. (2011) used a radar ensemble to generate ensembles of initial conditions and showed that the uncertainty from initial conditions decays within the first 48 h of the forecast. Another very challenging issue is the uncertainty about the distribution and intensity of the main triggering variable, the precipitation. It is already challenging to estimate precipitation distributions spatially when precipitation has occurred, but even more difficult to predict its spatial and temporal distribution in advance to be

able to issue warnings and take preventive actions if needed to minimise any kind of loss. In flood prediction meteorological uncertainty is therefore usually assumed to be the largest source of uncertainty (Rossa et al., 2011). Precipitation data to drive the hydrological model normally stems from either rain gauges, weather radar or numerical weather prediction systems, all having their advantages and disadvantages.

Precipitation measurements from rain gauges are very accurate at the point scale (Villarini et al., 2008). However, they cover only small areas of a few square decimetres (Michelson, 2004; Sevruk, 1996) but are then interpolated over tens or hundreds of square kilometres (Tobin et al., 2011; Velasco-Forero et al., 2009). Considering the very high spatial variability of precipitation, a problem of representativeness arises. Ensemble generators based on observed rain-gauge data are approaches to deal with these uncertainties (e.g. Ahrens and Jaun, 2007; Moulin et al., 2009; Rakovec et al., 2012).

The weather radar quantitative precipitation estimate (QPE) seems to be a very suitable product to detect the location of precipitation and to follow its development over time very closely because it is available at very high spatial and temporal resolutions. In Switzerland the information is provided every 5 min at a spatial resolution of 1 km (Germann et al., 2006). However, determining weather radar QPE is not an easy task, particularly in mountainous terrain, due to various sources of error, such as beam shielding, ground clutter and hardware instabilities, etc. (Germann et al., 2006; Szturc et al., 2008; Werner and Cranston, 2009). One approach to take these uncertainties into account is to use ensembles of weather radar QPEs (Germann et al., 2009; Liechti et al., 2013). This approach is also followed in the present study by using the probabilistic real-time radar nowcasting tool REAL (Radar Ensemble generator designed for the Alps using LU decomposition) developed by MeteoSwiss (Germann et al., 2009). But like rain-gauge data, radar QPEs are only available in real-time and not in advance.

A common way to predict precipitation is to use numerical weather prediction systems (NWP). They are run at different spatial and temporal resolutions, typically ranging from about 2 to 20 km and from 24 to 240 h of lead time (Montani et al., 2011; Zappa et al., 2008; Price et al., 2012a). One of the most detailed models available in Europe is the COSMO-2, which has a grid size of 2.2 km and 24 h of lead time computed every 3 h (Weusthoff et al., 2010; Ament et al., 2011). For NWP rainfall forecasts the largest source of uncertainty is found in the initial conditions of the NWP model (Price et al., 2012a). To account for this uncertainty ensemble forecasts are produced by adding small perturbations to the best estimate of the initial state of the atmosphere (Schellekens et al., 2011).

These sources of precipitation estimates are all used as input in hydrological modelling. As an example, Price et al. (2012b) present a flood forecasting system for England and Wales forced by the radar-based rainfall product STEPS

(control run) (Bowler et al., 2006) during the first hours of the forecast, followed by different NWP products with different lead times (36–120 h) and spatial resolutions (4–25 km). They conclude that despite the errors encountered in radar rainfall data, these are still the best option for real-time forecasting. However, to forecast rapidly responding catchments accurate and reliable merged products of radar and rain-gauge data will play an essential role in the future. Up to now, for flash-flood early warning purposes, weather radar data is mainly used as input for nowcasts with zero lead time (Germann et al., 2009; Liechti et al., 2013; Zappa et al., 2011), which are then only meaningful within the response time of the modelled catchment, as Morin et al. (2009) describe. They developed and tested a flash-flood warning model for two catchments in the Dead Sea region based on real-time radar data. The system operates in both deterministic and probabilistic mode. For the probabilistic nowcasts they applied Monte Carlo simulations with an uncertainty range for both the radar QPEs and the model parameters. Despite the large amount of uncertainty they obtained acceptable model performance with their nowcasting system. For smaller catchments prone to flash floods, however, the response time of the catchment may be too short to issue useful warnings and to take mitigation actions in good time.

To give radar-based forecasts with a more useful lead time, methodologies based on Eulerian and Lagrangian persistence can be applied to the radar data. Eulerian persistence keeps the current radar image frozen as a forecast for the near future (Germann and Zawadzki, 2002), while the Lagrangian persistence basically extrapolates the past motion of the precipitation into the future (Germann and Zawadzki, 2004; Mandapaka et al., 2012). Berenguer et al. (2005) did a hydrological verification of a radar-based nowcasting system by comparing stream-flow forecasts driven by S-PROG data (Seed, 2003) with forecasts driven by Eulerian and Lagrangian persistence. S-PROG is a simple extrapolation technique, based on Lagrangian persistence, that assumes a steady state for the motion of the rainfall field and also filters out the small-scale patterns of the rainfall field as the forecasting time increases. The verification of the system showed that an improvement in the precipitation forecast could be achieved with this method. However, the improvements in hydrograph prediction were not significantly better with S-PROG than with the simpler Lagrangian persistence.

To extend the lead time for flash-flood and flood early detection, several studies have also investigated the application of NWP forecasts in flash-flood and flood early warning systems. Schellekens et al. (2011) report good results for operational flood forecasts across the Thames Region using the MOGREPS ensemble forecasting system (Bowler et al., 2008) developed by the Met Office. Addor et al. (2011) compared flood forecasts driven by probabilistic and deterministic NWP forecasts. In their case study they found that, despite the coarser spatial resolution, the probabilistic forecast outperforms the deterministic forecasts for the whole forecast

range of three days and also extends the lead time. Similarly, Alfieri et al. (2012) analysed the performance of a NWP-driven flash-flood alert system. They used a 30 yr meteorological re-forecast (Fundel et al., 2010) to derive warning thresholds from the hydrological model with the aim to be independent from any stream-flow observations. They calculated forecasts every third hour at a spatial resolution of 1 km with lead times up to 5 days and analysed their flash-flood forecasting system on the basis of a qualitative and quantitative performance analysis of the Verzasca Catchment in southern Switzerland. The problems they encountered are well known: (1) only a limited amount of data is available for verification, which is why the warning thresholds are set very low to be able to do robust statistics, but these thresholds are then not really relevant for flash floods; (2) the catchment reacts very quickly to extreme precipitation and thus the interval at which the model operates is a limiting factor; and (3) NWP forecasts of convective precipitation events are not very accurate. To address this last issue, Rossa et al. (2010) tested a hydro-meteorological forecasting chain that assimilates radar rainfall data into the NWP model COSMO-2 prior to processing the forecast data with a hydrological model. This allows the main convective systems to be introduced into the model state, which enhances the timing and localisation of precipitation forecasts. This method seemed to improve discharge forecasts up to a lead time of three hours.

Up to now flash-flood early warning systems have either been run with NWP or, if run with weather radar data, they have been restricted to nowcasts with very limited lead time. Most of these studies, however, applied a deterministic approach. The study presented here is an incremental contribution to Zappa et al. (2011) and Liechti et al. (2013). In Zappa et al. (2011) the superposition of different sources of uncertainties in the hydro-meteorological forecast chain was investigated. In Liechti et al. (2013) the radar ensemble product REAL and a parameter ensemble approach were tested for hydrological nowcasting. Here we intend to go beyond nowcasting and move towards radar-based flash-flood forecasting by extending the lead time and in applying two novel approaches of radar-based ensemble flash-flood forecasting. The first one is purely radar-based and provides forecasts for the next eight hours. It propagates analogue-based weather radar forecasts with a hydrological model and is designed for situations with orographic precipitation. The other approach combines the real-time radar ensemble nowcast REAL (Germann et al., 2009) with the numerical weather prediction model COSMO-2. The resulting stream-flow forecasts are analysed and compared to deterministic radar-based forecasts. A pluviometer-based forecast chain additionally serves as a reference forecast, as rain-gauge data was used for the calibration of the hydrological model. The aim of our study is to investigate the potential of radar-based ensemble flash-flood forecasts with special emphasis on purely radar-based flash-flood forecasts. The experiments comparing the results of the different radar-based forecasting chains

highlight the value of ensemble forcing and the positive influence of using an ensemble of initial conditions for flash-flood early warning with lead times up to eight hours. Three basins of different sizes in the southern Swiss Alps were analysed, including the well-investigated Verzasca River basin (Alfieri et al., 2012; Germann et al., 2009)

2 Material and methods

2.1 The hydrological model

All the discharge forecasts in this study were produced with the semi-distributed rainfall-runoff model PREVAH (Gurtz et al., 2003; Viviroli et al., 2009a). The model is used in operational mode in many Swiss catchments for hydrological forecasting, amongst others in the catchments presented in this study. PREVAH operates at a spatial resolution of 500 m; however, this grid is assembled to hydrological response units (HRU) containing information on land use, soil and topography (Gurtz et al., 2003). The model is set up to work at hourly intervals. This allows a direct comparison of the different forecast chains, as the meteorological input from COSMO-2 also has a temporal resolution of one hour. Also regarding the response time of the study catchments this temporal resolution is sufficient. The meteorological variables required to run the model are air temperature, water vapour pressure, global radiation, sunshine duration, wind speed, and precipitation. Due to the topographical variation in the catchments, an altitude-dependent gradient has to be considered for air temperature, wind speed, water vapour pressure and global radiation (Jaun and Ahrens, 2009; Viviroli et al., 2009a; Zappa and Kan, 2007).

The model is calibrated using meteorological data from automatic ground stations. This data is interpolated with inverse distance weighting to form meteorological surfaces on a 500 m \times 500 m grid (Viviroli et al., 2009b). The 14 adjustable parameters of the PREVAH model used in this study originate from a default calibration for the Verzasca Catchment obtained from previous applications (Ranzi et al., 2007; Wöhling et al., 2006). The most sensitive parameters are the two water balance adjustment terms used to account for systematic correction of liquid and solid precipitation input (Viviroli et al., 2009b). As discussed in Viviroli et al. (2009b), such systematic correction is introduced to account for the integral discharge volume error arising from different sources (most prominently: under catch of precipitation gauges, rain gauge network representativity, interpolation errors, estimation of evapotranspiration and even bias in the runoff observations). The aim of the calibration was to find the parameter set that simulates the average flow best and that has the smallest volume error between the observed and simulated time series (Viviroli et al., 2009a; Zappa and Kan, 2007). For this purpose nine objective functions focussing on high flows, low-flow, average-flows and discharge volume

are combined (Viviroli et al., 2009b). A 13 yr data record was used for model calibration and verification. The year 1992 was used as the initialisation period for the model, the years 1993 to 1996 for the calibration period and 1997 to 2004 for the verification period.

In the presented study we also used precipitation estimates from weather radar and NWP to force the hydrological model. Due to the lack of homogeneous time series long enough to perform a calibration, the weather radar data was used without a water balance adjustment. Prior to being used by PREVAH, the radar and NWP fields need to be down-scaled to meet the spatial resolution required by PREVAH (Jaun et al., 2008). Discharge time series for verification were provided at hourly intervals by the Federal Office for the Environment (FOEN).

2.2 Data

The precipitation nowcasts and forecasts used in our forecasting chains are described in the following sections. The methodologies we used have already been described in detail in previous publications. For details about the retrieval of weather radar and NWP products, see the articles cited below.

2.2.1 NORA – Nowcasting of Orographic Rainfall by means of Analogues

As precipitation in mountainous regions is influenced by orographic forcing, Panziera and Germann (2010) investigated the effects of orographic forcing on the rainfall patterns in the Lago Maggiore Region in southern Switzerland (Fig. 1). They found strong relationships between the precipitation patterns and wind intensity, and the wind direction and air-mass stability present under orographic forcing. Based on this finding, they developed NORA (Nowcasting of Orographic Rainfall by means of Analogues), an analogue-based heuristic nowcasting system to predict orographic rainfall for the following eight hours (Panziera et al., 2011). It involves finding earlier observations very similar to the current situation with respect to predictors describing the orographic forcing (four different mesoscale flows and air-mass stability) and two features of the radar rainfall field (fraction of rainy area and average rainfall). To speed up the process of finding analogues, all past weather radar data is reduced to an archive that only contains situations related to orographic forcing. This archive was produced according to three different requirements: (1) the archive should be large enough to cover the whole range of the phenomena of interest; (2) it should be homogenous in terms of instrumental changes and data-processing techniques; and (3) the events selected should be long-lasting and widespread, as typically caused by large-scale supply of moisture towards the Alps. Isolated convection and air-mass thunderstorms were excluded from the archive. All these criteria finally resulted in an archive of

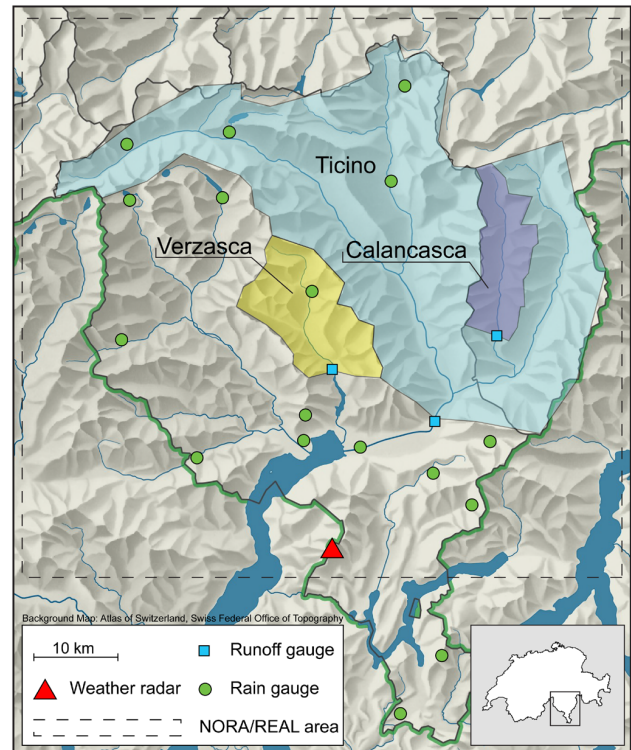


Fig. 1. Lago Maggiore region, southern Switzerland, with test catchments, meteorological and hydrological stations and weather radar used in this study. The rectangle with dashed lines shows the area for which NORA and REAL have been produced.

71 precipitation events observed between January 2004 and December 2009, corresponding in total to 3050 h of rainfall.

To produce the NORA forecast, the historical situations most similar to the current one are searched for in the archive. This procedure is divided into two steps. In a first step, the 120 past instances most similar in terms of meteorological predictors (four mesoscale flows and air-mass stability) are chosen (forcing analogues). In a second step, the 12 analogues that, among the 120 forcing analogues, have the rainfall pattern most similar to the current one are picked. They constitute the final analogues. The NORA forecast is then produced according to the rainfall fields observed in the eight hours following each of the final analogues. This results in an ensemble of 12 members, one of which will, by construction, always be Eulerian persistence (Fig. 2). In this study, the number of forcing and final analogues of NORA was fixed, but in general it can be changed according to the archive size and the application. NORA is produced only if at least one of the four mesoscale winds can be estimated. Otherwise no orographic forcing is expected, and thus no NORA forecast is issued. The technical details about the algorithms behind NORA are given in Panziera et al. (2011). NORA forecasts were originally issued in 5 min time steps, but were aggregated to hourly time steps for our study. This may reduce the

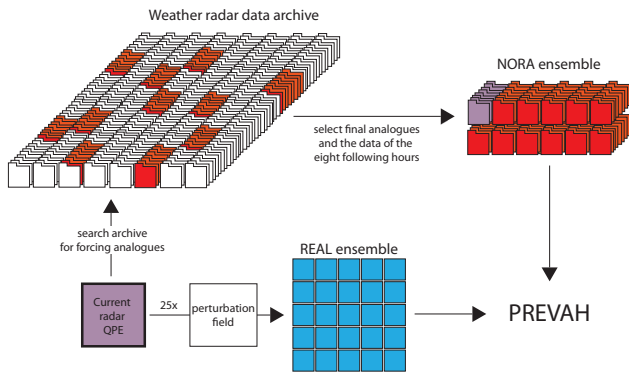


Fig. 2. Procedure to build the ensembles REAL and NORA. For the REAL ensemble, the current radar QPE is perturbed by a perturbation field 25 times to build an ensemble of 25 members. To build the NORA ensemble, a radar data archive is searched to find the situations most similar to the current radar QPE. Then those analogues and the data of the eight hours following each forcing analogue are extracted from the archive, and an ensemble of 12 members with 8 h lead time each is built.

actual potential of NORA in forecasting timing and magnitude of flash-flood events, but is a trade-off for the comparability with the other forecast chains and the computability in an operational context. For the past events analysed in this study, the whole archive was searched for analogues. This meant that a hindcast of an event could also contain analogue situations that actually took place after the considered event in the past. Therefore, the 24 h following the initialisation of each NORA forecast were excluded from the archive in which the analogues were sought. Panziera et al. (2011) found that the results produced in this way did not differ significantly from results produced when only the hours of the archive preceding the NORA forecasts were included.

2.2.2 REAL – radar ensemble

REAL (Radar Ensemble generator designed for the Alps using LU decomposition) was developed by MeteoSwiss as a probabilistic real-time radar nowcasting tool (zero lead time). It provides an ensemble of 25 members, each of which results from the sum of the current radar image and a stochastic perturbation field (Fig. 2). This perturbation field is a combination of stochastic simulation techniques and detailed knowledge about the space-time variance and auto-covariance of radar errors (Germann et al., 2009). To obtain this knowledge, a suitable network of meteorological ground stations is required. With this methodology the residual space-time uncertainties of the radar precipitation estimates are accounted for. REAL has been produced since May 2007 at hourly intervals with a spatial resolution of $2\text{ km} \times 2\text{ km}$ (Germann et al., 2009) for the Lago Maggiore region in the southern Swiss Alps (Fig. 1).

2.2.3 Connection of REAL and COSMO-2

For our study we connected COSMO-2 forecasts to the radar-ensemble nowcasts of REAL. COSMO-2 (C2) is a deterministic numerical weather prediction (NWP) model of the Consortium for Small-scale Modelling (COSMO). It has a lead time of 24 h, a spatial resolution of 2.2 km and has been issued every three hours (00:00, 03:00, 06:00, 09:00, 12:00, 15:00, 18:00, 21:00 UTC) since the beginning of demonstration period of MAP D-PHASE (Rotach et al., 2009) in June 2007. The connection with REAL implies that COSMO-2 meteorological input is actually propagated through the hydrological model every hour with 25 different initial conditions stemming from the nowcast obtained by forcing PREVAH with REAL.

2.2.4 Deterministic forecasts

In addition to the two ensemble forecast chains with NORA and REAL-C2, we also tested the performance of two deterministic model chains. They are constructed like the REAL-C2 forecasts, but unlike with REAL, the initial conditions are derived by driving PREVAH with the deterministic weather radar QPE (RADAR) or interpolated rain-gauge data (PLUVIO). The data for the interpolated precipitation surfaces originated from automated rain-gauge stations, which have a temporal resolution of 15 to 30 min. These were aggregated to hourly values and interpolated with inverse distance weighting over the areas of the test catchments on a $500\text{ m} \times 500\text{-m}$ grid. Additionally, a bias correction factor was determined by calibration (Zappa and Kan, 2007) and applied to all interpolated values, in order to minimise the total discharge volume error at the catchment outlets (Viviroli et al., 2009a). The radar QPE was taken from the weather radar on Monte Lema (Fig. 1). They are available at a temporal resolution of five minutes and at a spatial resolution of 1 km^2 , but were aggregated to hourly time steps and downscaled to a $500\text{ m} \times 500\text{-m}$ grid.

COSMO-2 takes 2.5 h to assimilate, compute and disseminate. Since COSMO-2 is produced every three hours, this means that the COSMO-2 forecast is three to five hours old by the time it can be used for the hydrological forecast.

Table 1 shows the schedule for connecting COSMO-2 forecasts to nowcasts forced by REAL, RADAR or PLUVIO.

2.2.5 Study period

The beginning of the study period was set to June 2007 according to the availability of COSMO-2. December 2010 defines the end of our study period. Due to the replacement of the weather radar on Monte Lema (Fig. 1), the continuous and homogeneous series of high quality weather radar data ends in early summer 2011. For the period June 2007 to December 2010, NORA forecasts were initialised on 1389 h, when orographic precipitation occurred. These 1389 h were

Table 1. COSMO-2 forecasts connected to discharge nowcasts forced by REAL, deterministic radar QPE (RAD) and interpolated rain-gauge data (PLU). Times are in hours UTC.

Initialisation of COSMO-2 forecast	Available at	Start of discharge forecast
00:00	02:30	03:00, 04:00, 05:00
03:00	05:30	06:00, 07:00, 08:00
06:00	08:30	09:00, 10:00, 11:00
09:00	11:30	12:00, 13:00, 14:00
12:00	14:30	15:00, 16:00, 17:00
15:00	17:30	18:00, 19:00, 20:00
18:00	20:30	21:00, 22:00, 23:00
21:00	23:30	00:00, 01:00, 02:00

distributed over 40 events. We analysed all 1389 forecasts, each of which consists of eight hours, for all forecasting chains included in our study. The 40 individual events are plotted sequentially in Fig. 3 for the Verzasca Catchment, as an example, along with the NORA and REAL-C2 forecasts for 3 and 6 h lead time.

2.3 The catchments

Catchments were selected in the Lago Maggiore region in southern Switzerland, where NORA and REAL are available. Until today these two products have been specially produced for research purposes and are therefore only available for this limited region (Fig. 1). In many catchments in the region, water is intensively managed for hydropower production. We therefore selected two smaller catchments which are not, or only slightly, affected by water management, as well as a large catchment to explore the effects of scale.

The Calancasca Catchment is 120 km² and the smallest of the three catchments. The Calancasca valley is a sub-catchment of the Ticino catchment, and is very rural and mountainous with steep slopes ranging from 740 m a.s.l. to 3200 m a.s.l. in altitude. At the top of the catchment a small glacier is covering 1.1 % of the catchment area. The catchment is little affected by hydropower, but some of the headwater is partly redirected to a hydropower plant in the neighbouring catchment to the east. This diversion is taken into account in the hydrological model with the routing module. Downstream of the Calancasca gauge, the stream water is stored in a small retention lake for hydropower production.

The Verzasca Catchment is 186 km² in area ranging from 490 to 2900 m a.s.l. It is very little influenced by human activity. At altitudes above the discharge gauge in Lavertezzo it is not affected by any water management but below the gauge, the river Verzasca flows into Lago di Vogorno, a retention lake for hydropower production. The basin is the main focus area for our research group. Wöhling et al. (2006) presented the results of model calibration and introduced an assimilation procedure aimed at improving the quality

of initial conditions prior to and during an event. Zappa et al. (2011) developed and tested a methodology to quantify the relative contribution of different sources of uncertainty (forcing, initial conditions and model parameter estimation) to the total uncertainty of a real-time flood forecast. Germann et al. (2009) and Liechti et al. (2013) focused on the verification of the use of REAL as a forcing for real-time nowcasts. The present study is an incremental contribution, that goes beyond nowcasting. The connection of nowcasts with COSMO-2 and the novel radar-based ensemble forecast NORA allow us to investigate flash-flood forecasts with some hours lead time.

The Ticino catchment is 1515 km² in area. It is much more densely populated and thus more influenced by human activity than the two small catchments. The main valley of the Ticino catchment is part of one of the main transit routes that crosses the Alps. Hence the lower area of the catchment, where the valley is broad enough, is intensively used for industry and agriculture, whereas the steep slopes are only little used. Altitudes range from 220 m to 3400 m a.s.l. The influence of water management is substantial, but all water remains in the catchment and reaches the gauge in Bellinzona.

2.4 Experimental set-up

Our experimental set-up in hindcast mode for the five different forecasting chains consisted of a nowcasting part with zero lead time (realtime) and a forecasting part (Fig. 4). The nowcasting part was initialised five days prior to the onset of the NORA forecast (t_0) by the model state derived from a reference run forced by pluviometer data (Fig. 4). This real-time part was run for four days, which meant the influences of the initial model state are reduced at the start of the forecasting part at time t_0 . The five forecasting chains analysed are

1. NORA: NORA forecast initialised by a deterministic RADAR nowcast.
2. PERS: the persistence of the current radar QPE at time t_0 (i.e. taking the signal of t_0 for the next eight hours) initialised by a deterministic RADAR nowcast.
3. REAL-C2: COSMO-2 forecast initialised by a probabilistic REAL nowcast.
4. RAD-C2: COSMO-2 initialised by a deterministic RADAR nowcast.
5. PLU-C2: COSMO-2 initialised by a deterministic PLUVIO nowcast.

In comparing the performance of REAL-C2 and NORA to RAD-C2 we can illustrate differences between probabilistic and deterministic forecasts. The three main experiments resulting from this comparison are

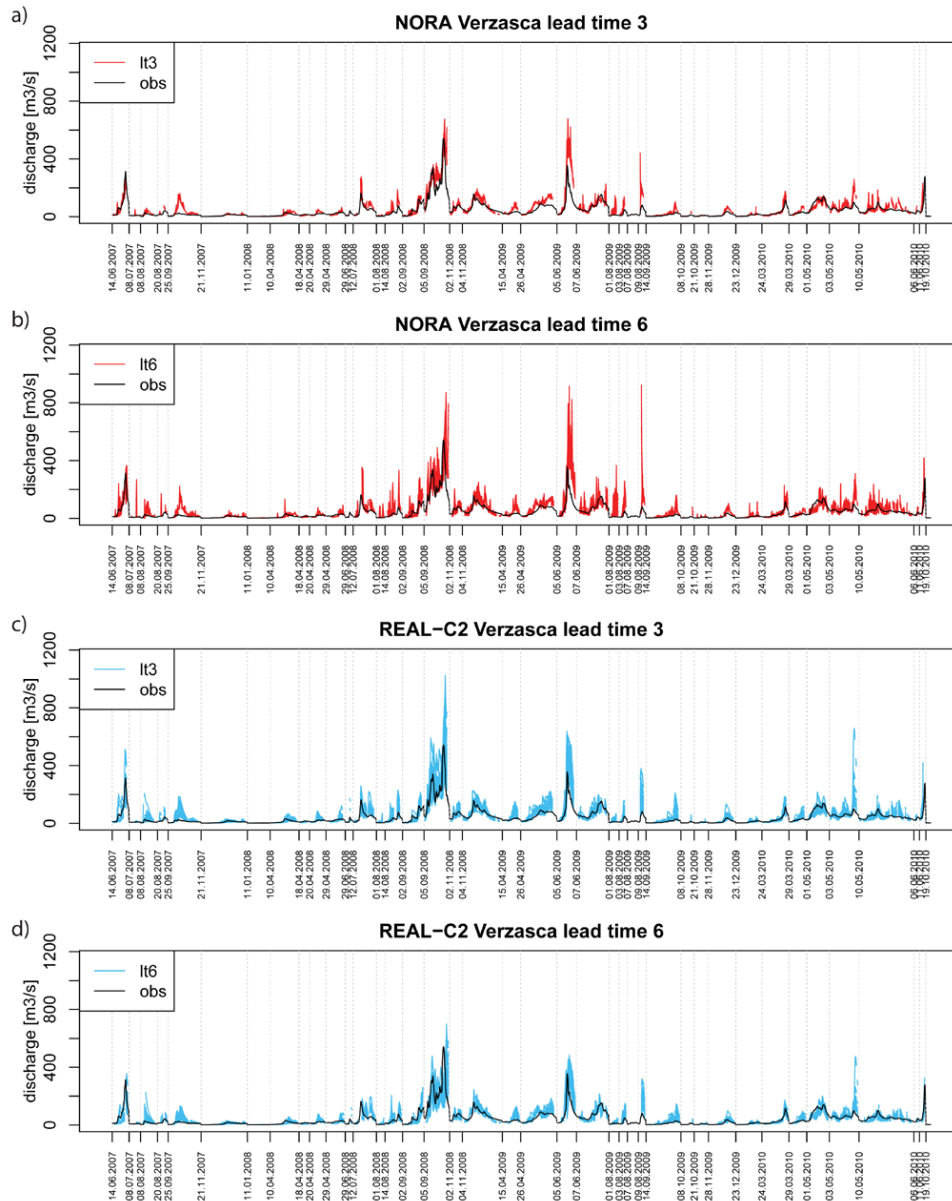


Fig. 3. NORA and REAL-C2 discharge ensemble for the Verzasca River for all 40 events in the study period. The panels (a) and (c) show the discharge ensembles at 3 h lead time, and the panels (b) and (d) show the discharge ensembles at 6 h lead time. The individual events are separated by dashed vertical lines. The dates given in the x axis refer to the date of the beginning of each event.

1. NORA vs. RAD-C2, showing the effect of ensemble forcing.
2. REAL-C2 vs. RAD-C2, showing the effect of an ensemble of initial conditions.
3. NORA vs. REAL-C2, setting the two ensemble forecasting chains in relation to each other.

The comparison of PERS with the other forecast chains shows if there is actually any benefit in producing a forecast. The PLU-C2 forecasting chain stands for itself and has

to be seen as a reference. Compared to the radar-based forecasting chains this chain has an advantage due to the fact that the hydrological model was calibrated using rain-gauge data. The diagram in Fig. 4 visually explains the different model chains and introduces the names and the colour scheme used from now on for the different forecasting chains.

2.5 Verification methods

As NORA is limited to a lead time of eight hours, we concentrated our verification on these eight hours. We analysed the

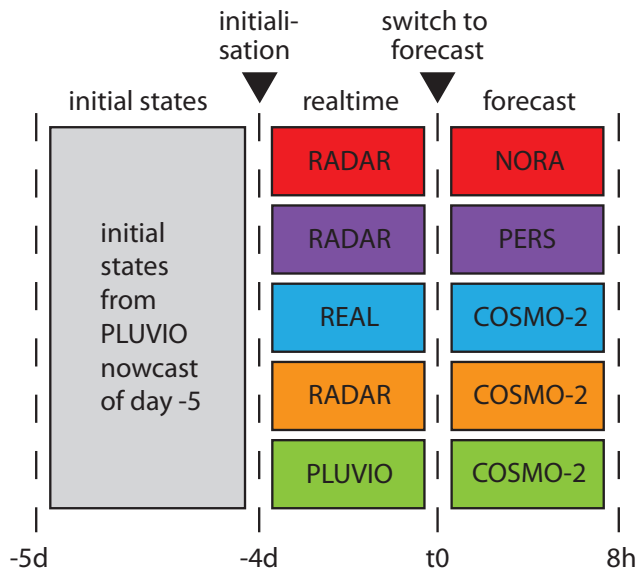


Fig. 4. Diagram showing the different forecasting chains. From the top: NORA, PERS, REAL-C2, RAD-C2 and PLU-C2.

performance of the different forecasting chains for each lead time (1–8 h) separately, as well as for six different thresholds with the following measures of skill:

The *Brier skill score* (BSS) is an ideal measure to compare the performance of probabilistic and deterministic forecasts (Wilks, 2006). The BSS is based on the Brier Score (BS), which describes the quality of the forecast system in predicting the probability to exceed a predefined threshold by measuring the squared probability error. A perfect forecast system would have a BS of zero. In order to compare the different forecast systems to each other, we made use of the BSS, which sets the skill of the different forecasts in relation to a reference forecast. A perfect forecast has a BSS of 1, whereas forecasts worse than the reference forecast have a skill below 0. In our study, the reference forecast was the probability of exceedance for the predefined thresholds based on the sample climatology. The sample incorporated all discharge observations from hours covered by one or more NORA forecasts. This resulted in a sample size of 1788 h. The thresholds analysed in our study correspond to the 0.5, 0.6, 0.7, 0.8, 0.9 and 0.95 quantile of the sample climatology, which we refer to as q50, q60, q70, q80, q90 and q95. As the sample is restricted to the hours covered by NORA, the actual values of the thresholds quantiles are higher than the ones used in our previous study (Liechti et al., 2013). To estimate the uncertainty of the BSS values, we applied the bootstrapping method (Efron, 1992). Thus 500 random samples of forecast-observation pairs were drawn with replacement from the 1389 h belonging to each lead time leading to the confidence limits (95 %) shown in Fig. 5.

The *False Alarm Ratio* (FAR) and *Probability Of Detection* (POD) are interlinked and therefore shown together. Both are

measures to evaluate deterministic predictions, where the ensembles were reduced to their medians. FAR is the fraction of the forecast threshold exceedances that turn out to be wrong. The best FAR value is zero, which means that each positive forecast was followed by a threshold exceedance. POD is the ratio of correctly forecast threshold exceedances to the number of times the event really happened. The best POD value is one, which means that each observed threshold exceedance was forecast. The POD is only sensitive to missed events and not to false alarms, and thus can always be improved by forecasting an event more frequently. This would, however, lead directly to an increase in false alarms and would, for extreme events, result in an overforecasting bias (Bartholmes et al., 2009; Wilks, 2006).

The *ROC area* (ROCA) is the area under the ROC (relative operating characteristic) curve. A ROC curve is drawn in a ROC diagram, which incorporates information on the POD (y axis) and the false alarm rate (x axis) for the whole range of forecast probabilities. The false alarm rate is the fraction of non-occurrences for which a threshold exceedance was forecast. A perfect forecast will result in a ROC curve connecting the points (0/0), (0,1) and (1/1) of the ROC diagram. An unskilful forecast will not lie above the diagonal (0/0),(1,1). Thus the area under the ROC curve is a convenient way to express the degree of discrimination. ROC is not, however, sensitive to an overall bias, which means that ROC actually indicates the potential skill that would be achieved if the forecasts were correctly calibrated (Wilks, 2006). Therefore we also show the bias of the different forecasting chains.

3 Results

First we show how the spread of the two ensembles NORA and REAL-C2 generally develops over lead time. We then present the results for the three catchments separately. The results of the analysis with ROC area are summarised for all catchments together. Finally, we present a forecast for the Calancasca as it appears in operational mode.

3.1 Chained time series

In Fig. 3 all events in the study period are plotted sequentially together with the forecasts with 3 and 6 h lead time for the Verzasca Catchment. The spread of the NORA ensemble increases with the lead time for all catchments; however, the spread of the REAL-C2 ensemble behaves differently in the Verzasca Catchment than in the Ticino and Calancasca catchments. In Ticino and Calancasca the spread of the REAL-C2 ensemble stays about constant over the eight hours analysed (not shown), but in the Verzasca Catchment the spread of REAL-C2 decreases with longer lead times. This is possibly due to the nature of the events included in the study period and is further discussed in Sect. 4.3.1. For the Ticino

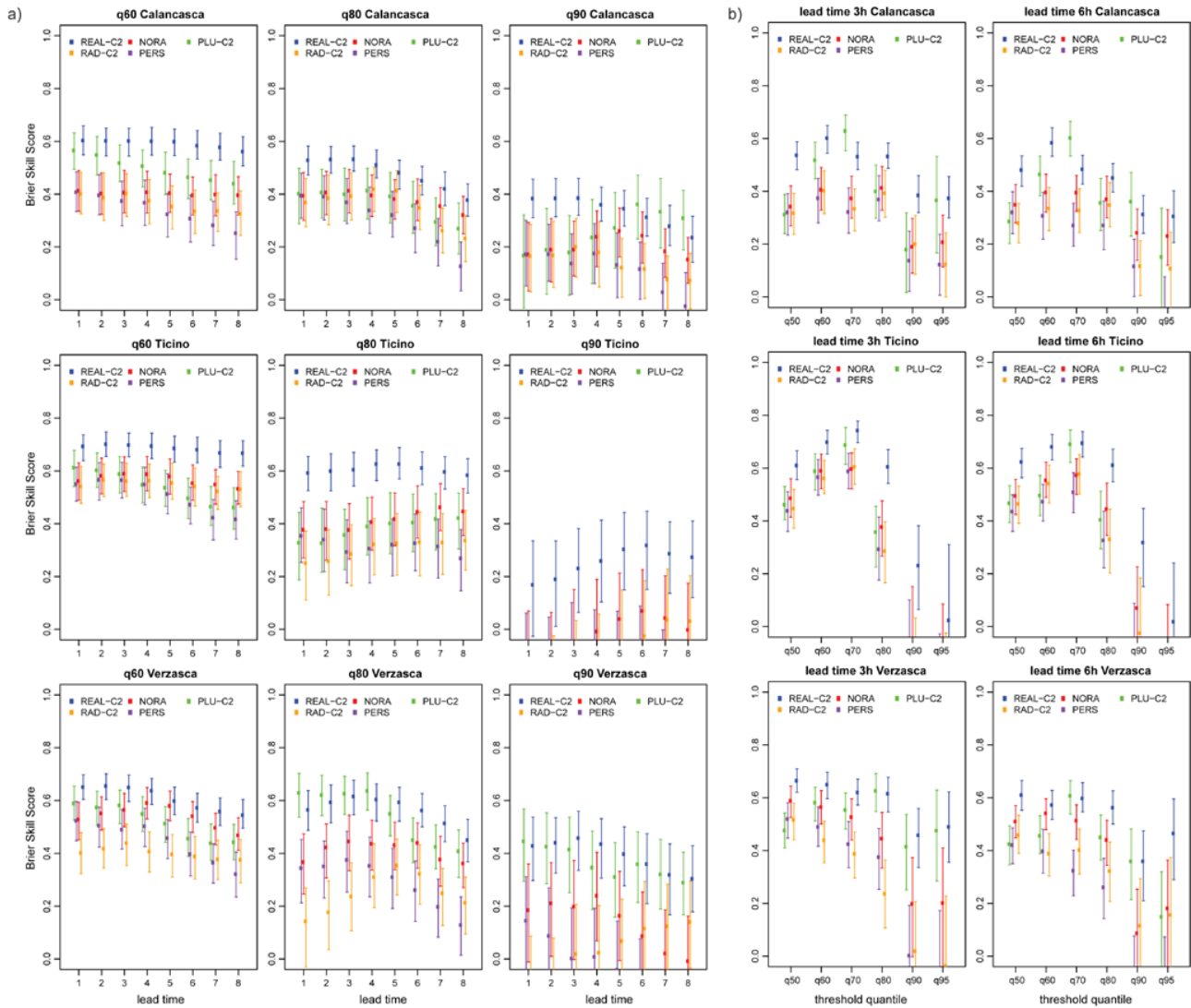


Fig. 5. (a) Brier skill score (BSS) according to lead time for the threshold quantile q60, q80 and q90. (b) BSS according to the threshold quantiles q50 to q95 for 3 and 6 h lead time. Error bars indicate the 95 % confidence limits around the estimated BSS value. Positive BSS values indicate an improvement in the forecast over the reference forecast, which in this case is the sample climatology.

and Calancasca catchments the spread of REAL-C2 is larger than that of NORA for all lead times, although for Calancasca the difference is relatively small from 6 h lead time on. For Verzasca, the spread of REAL-C2 is only larger than that of NORA for up to 4 h lead time, and from 6 h lead time onwards NORA forecasts have a larger spread than REAL-C2 forecasts.

3.2 Calancasca

BSS values for REAL-C2 generally decrease with increasing threshold and longer lead times. REAL-C2 shows skill on all thresholds and all lead times. The highest BSS values are reached with q60 (0.56–0.6), but for q90 and q95 BSS values are still as high as 0.35 to 0.4 (Fig. 5b). NORA shows

lower scores than REAL-C2, and its BSS values range between 0.35 to 0.4 for q50 to q80. For the highest thresholds BSS values are lower, while for q90 and q95 they range between 0.15 and 0.25. BSS values for PERS clearly decrease with lead time (Fig. 5a). The highest score is reached at q60. BSS values for q90 and q95 are below 0.2, while q90 shows no skill for lead time 8 (Fig. 5a) and q95 shows no skill after 3 h lead time (Fig. 5b). RAD-C2 also shows skill on all thresholds and lead times, but this decreases with lead time (Fig. 5a). RAD-C2 forecasts reach BSS values between 0.3 and 0.4 for q60 to q80 and lead times up to 6 h. The performance on q70 and q80, however, fall below 0.3. For q90 and q95 BSS values are generally lower than 0.2 (Fig. 5b). BSS values for PLU-C2 are highest on q70 and are above 0.6 up to 6 h lead time. Additionally PLU-C2 outperforms

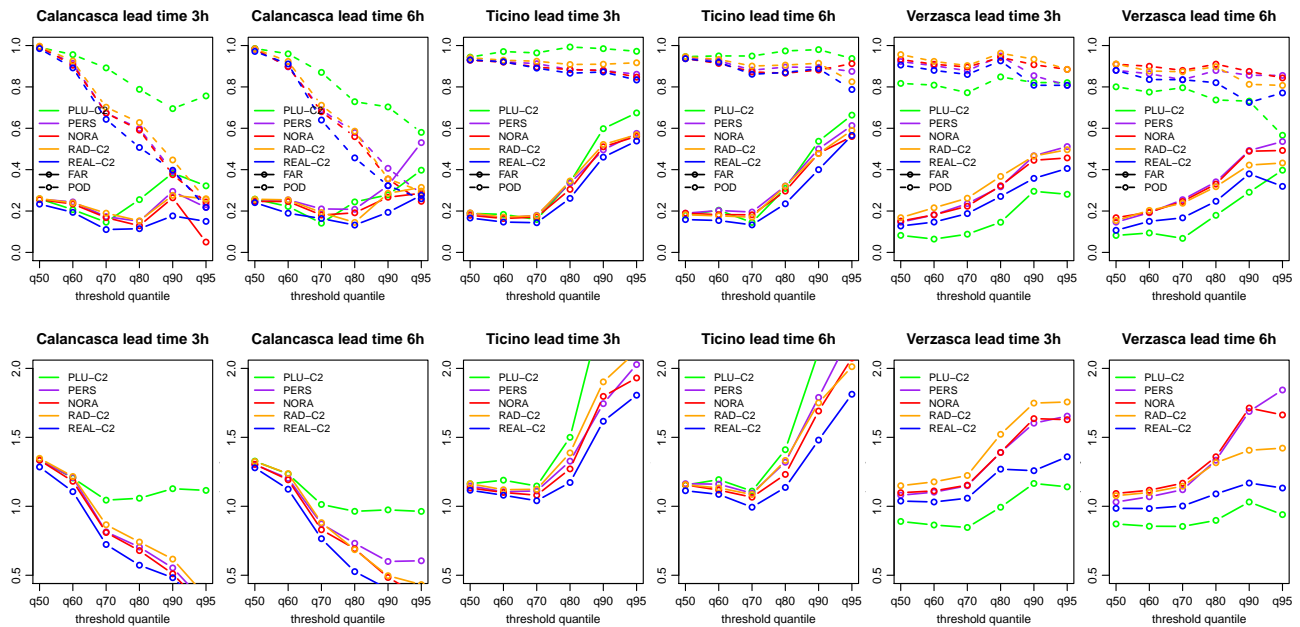


Fig. 6. Probability of detection (POD, dashed line), false alarm ratio (FAR, solid line) and BIAS (lower panel) for each catchment for the thresholds q50 to q95 with 3 and 6 h lead time. Best FAR equals 0, best POD and BIAS equals 1.

all other forecast chains on this threshold. For the highest quantile PLU-C2 also shows skill over all lead times, varying between 0.14 and 0.36.

The probability of detection (POD) for PLU-C2 is higher than for the other forecast chains, as are the FAR values for thresholds q80 to q95 (Fig. 6). POD and FAR for PLU-C2 behave symmetrically from q70 to q95, which is not the case for the other forecast chains. POD for REAL-C2, NORA, PERS and RAD-C2 rapidly decrease above q60. FAR are lowest for REAL-C2 on all quantiles except q95. FAR and POD for NORA, PERS and RAD-C2 are about the same. FAR values range between 0.1 and 0.3 and POD values drop from 0.9 at q60 to 0.2–0.3 at q95. If we increase the lead time from 3 to 6 h, the main difference is with the q95 threshold, where the FAR values are highest for all forecasting chains (Fig. 6). The different behaviour of the different forecasting chains is also mirrored in the bias. Forecasts for Calancasca have an under-forecasting bias above q60 for all radar-based forecasts. The reasons for that can lie in model calibration but also in the size of the catchment, as for the relatively small Calancasca Catchment errors in the estimation of the location, duration and intensity of predicted rainfall do not smoothen until the catchment outlet. This is most pronounced for REAL-C2. PLU-C2 performs best and is hardly biased above q60. This behaviour does not change with increasing lead time.

3.3 Ticino

REAL-C2 reaches BSS values between 0.6 and 0.75 for thresholds between q50 and q70 for all lead times, but then drop significantly, ranging between 0.2 and 0.3 for q90

(Fig. 5b). Furthermore, for q95 REAL-C2 only shows skill for lead times 3 to 6, and even then is below 0.15, that is, very low. The highest scores for REAL-C2 are reached for q70 (Fig. 5b). For NORA the BSS values between q50 and q70 lay between 0.5 and 0.6 for all lead times. The highest scores are reached for q70. For q80 the values are a bit lower (0.35–0.45) and increase with lead time. For the highest thresholds NORA shows almost no skill. For PERS the highest BSS are reached for q70 at 1 h lead time (0.6). For both q60 and q70 scores for lead time 1 to 3 are between 0.55–0.6, but then BSS values decrease steadily to 0.4 at lead time 8. PERS show no skill on the highest quantiles (Fig. 5b). BSS values for RAD-C2 for q60 and q70 also range between 0.5 and 0.6, but decrease less with increasing lead time than PERS. For q80 BSS values increase from 0.25 at lead time 1 to 0.33 at lead time 8. Like PERS, RAD-C2 has no skill for q90 and q95 (Fig. 5b). BSS values for PLU-C2 for q50 and q60 decrease with lead time and range from 0.5 to 0.4 and 0.6 to 0.45, respectively. The highest scores are reached for q70 and range between 0.65 and 0.7. For q80 BSS values increase with lead time from 0.32 to 0.42. For the highest threshold quantiles, PLU-C2 shows no skill. For q50, q60 and q80 the skill of PLU-C2 is in the range of NORA and RAD-C2, but for q70 PLU-C2 outperforms all forecast types apart from REAL-C2. In comparison with all the other radar products REAL-C2, shows the most skill. The difference between NORA, PERS and RAD-C2 increases with increasing threshold and longer lead times. NORA performs better than PERS and RAD-C2 on the higher thresholds, but for PERS and RAD-C2 it depends on the lead time. At shorter lead

times, PERS scores better and on longer lead times RAD-C2 outperforms PERS.

POD values are high for all thresholds and forecast chains, ranging between 0.75 and 0.99. PLU-C2 shows the highest POD, RAD-C2 the second highest and REAL-C2, NORA and PERS about the same scores. FAR values behave differently and increase rapidly after q70 from about 0.15 to 0.55 and 0.7. Again PLU shows the highest FAR, REAL-C2 the lowest and the other forecast chains lie in between on about the same level. This matches with the bias obtained for the forecasts in the Ticino catchment. The bias is about 1–1.2 for q50 to q70, and then increases rapidly for all forecasting chains. PLU-C2 is the most biased and REAL-C2 the least over all thresholds. The same behaviour for bias, POD and FAR can be seen when looking at longer lead times, although the POD values for RAD-C2 on q95 are an exception as they are below those for NORA and PERS, and lower than at 3 h lead time.

The forecast chains are ranked in the same order for Ticino and Calancasca for POD and FAR, but the actual values of POD and FAR behave reversed, which is also mirrored in the overforecasting bias for the Ticino catchment. The reason for this overforecasting bias as well as for the increasing BSS with lead time is most probably the water management in the catchment, which causes that the rainfall of a storm does not reach the catchment outlet in the estimated time, but is stored or redirected and delayed.

3.4 Verzasca

Up to q80 BSS values for REAL-C2 are around 0.6, while for q90 and q95 they are between 0.4 and 0.5. The values generally decrease with increasing lead time. Values for NORA are lower than for REAL, and for q60 and q70, values range between 0.45 and 0.6 with a maximum at 4 and 5 h lead time. BSS values for q80 are around 0.4 with a maximum at lead time 3 (Fig. 5a). For q90 and q95, BSS values are around 0.2 up to lead times 5 and 6, but then decrease rapidly towards no skill. The persistence (PERS) starts from the same level as with NORA on the shortest lead times (BSS 0.55). However, the skill decreases with increasing threshold (Fig. 5b), and the decrease in BSS over lead time is faster for higher thresholds (Fig. 5a). BSS values for RAD-C2 decrease from 0.5 on q50 to 0.3–0.4 on q70. The BSS for short lead times on q80 are very low, but increase to a maximum of 0.35 for 5 h lead time. Similar to the persistence, q90 and q95 have no skill on the shortest lead times, however, BSS values show some skill for longer lead times. PLU-C2 reaches BSS values of around 0.6 for q60 to q80, which decrease with lead time (Fig. 5a). The highest BSS value for the shorter lead times (1–4 h) was reached with q80 (0.63). For the high thresholds, q90 and q95, BSS values still ranged between 0.4 and 0.5 for lead times of 1 to 3 h. If the radar products are compared, scores for NORA are generally below those for REAL, but above those of RAD-C2. For lead times 1 and

2, PERS outperforms RAD-C2 on high thresholds. However, for longer lead times RAD-C2 performs better than PERS. Comparing NORA with PLU-C2, we see that for q50 NORA still scores significantly higher than PLU-C2. This changes for q60 lead time 4, and from q70 onwards PLU-C2 shows better skill than NORA. This difference is most pronounced for short lead times.

All forecast chains show POD values above 0.8 on all thresholds. However, POD and also FAR values for PLU-C2 behave differently in the Verzasca Catchment than in the other two catchments. For Verzasca, PLU-C2 shows the lowest FAR and POD values of all forecast chains except q90 and q95, where REAL-C2 is a little bit lower in POD. FAR values generally increase with increasing threshold from about 0.15 to 0.4/0.5. REAL-C2 was the radar product that performed best. With increasing lead time, NORA outperforms RAD-C2 in POD. However, NORA also shows higher FAR values on thresholds higher than q60. Furthermore, for longer lead times, PLU-C2 reaches the lowest POD and highest FAR on q95 and not on q90, unlike for shorter lead times. Radar-based forecasting chains show a significant overforecasting bias for q80 to q95, which is most probably a calibration issue. PLU-C2 slightly underforecasts up to q70, and slightly overforecasts for q90 and q95. With increasing lead time, the bias for RAD-C2 becomes smaller for the high thresholds.

3.5 ROC area

The ROC areas presented in Tables 2–4 are generally higher than 0.7, which is considered to be the minimum value for a forecast system to be useful for a decision maker (Buizza et al., 1999). For Ticino and Verzasca, they do not drop below 0.9 up to q90. For Calancasca they are a bit lower, especially for NORA and for the high thresholds. For Calancasca and Ticino, the REAL-C2 forecasts have higher ROC areas than NORA forecasts on all lead times and thresholds, although this difference decreases with increasing lead time. For the Verzasca Catchment, the advantage of REAL-C2 over NORA is only clearly evident on short lead times. ROC areas for REAL-C2 decrease with lead time (except Ticino, q90), but this is not the case for NORA forecasts.

3.6 Forecast as in operational mode

In our analysis we focused on the performance of the different forecasting chains regarding specific thresholds and lead times. In an operational context the forecasts would be presented as shown in Figs. 7 and 8. Here the different forecasting chains are shown together and can be visually compared directly. The NORA forecasts are connected to COSMO-2 forecasts after eight hours, just as with the other forecasting chains at time t_0 . The examples in Figs. 7 and 8 show forecasts of an event in the Calancasca River on 15 June 2007 initialised prior to the event and during the event. The NORA forecast prior to the event gives a good estimate of the first

Table 2. ROC area for NORA and REAL-C2 forecasts of the Calancasca Catchment, with lead times 03:00, 06:00 and 08:00, for the threshold quantiles q60 to q95.

	Calancasca					
	lt3		lt6		lt8	
	nora	real	nora	real	nora	real
q60	0.874	0.935	0.877	0.929	0.879	0.924
q70	0.826	0.937	0.853	0.919	0.85	0.899
q80	0.817	0.945	0.839	0.923	0.826	0.899
q90	0.723	0.887	0.764	0.876	0.733	0.830
q95	0.652	0.897	0.736	0.838	0.725	0.825

Table 3. ROC area for NORA and REAL-C2 forecasts of the Ticino catchment, with lead times 03:00, 06:00 and 08:00, for the threshold quantiles q60 to q95.

	Ticino					
	lt3		lt6		lt8	
	nora	real	nora	real	nora	real
q60	0.911	0.962	0.913	0.959	0.914	0.958
q70	0.920	0.977	0.911	0.960	0.905	0.950
q80	0.902	0.968	0.914	0.967	0.917	0.955
q90	0.905	0.949	0.915	0.951	0.896	0.947
q95	0.934	0.971	0.944	0.968	0.925	0.946

Table 4. ROC area for NORA and REAL-C2 forecasts of the Verzasca Catchment, with lead times 03:00, 06:00 and 08:00, for the threshold quantiles q60 to q95.

	Verzasca					
	lt3		lt6		lt8	
	nora	real	nora	real	nora	real
q60	0.918	0.95	0.915	0.933	0.895	0.918
q70	0.916	0.954	0.923	0.935	0.904	0.911
q80	0.941	0.973	0.939	0.946	0.918	0.910
q90	0.934	0.967	0.911	0.922	0.887	0.888
q95	0.954	0.985	0.942	0.940	0.918	0.927

peak, which occurred seven hours after the forecast initialisation (t_0), but underestimates the main peak, which occurred 21 h after t_0 . The REAL-C2 forecast misses this first peak and also underestimates the second peak. For the forecast initialised during the event, however, NORA still underestimates the main peak, but REAL-C2 captures it.

4 Discussion

The skills of the different forecast chains, are easier to compare for lower thresholds as the results are clearer and more persistent over the catchments and lead times. Thus general conclusions about the performance of NORA and the other

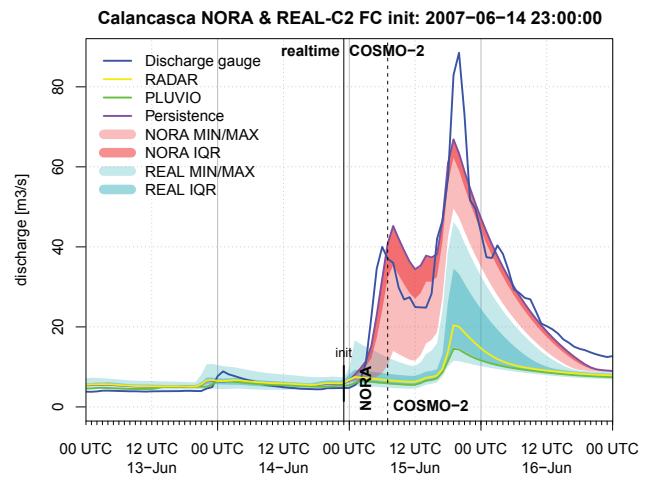


Fig. 7. Forecast simulation for the Calancasca initialised on 14 June 2007 at 23:00. At the time of the initialisation of NORA (vertical solid line), the nowcasts driven by REAL, RADAR and PLUVIO were connected to COSMO-2. After eight hours (vertical dashed line), NORA was also connected to COSMO-2. The analysis covers the eight hours covered by NORA forecasts, that is, the time frame between the vertical solid and dashed lines in the graph above.

forecasting chains can only be made for threshold quantiles up to q80. For higher quantiles the results vary considerably between the three catchments included in the study.

Panziera et al. (2011) verified NORA for precipitation thresholds of 0.5 and 3 mm per hour, which corresponds to a low threshold that distinguishes between rain and no rain, and a threshold for moderate to heavy rainfall. They integrated their analysis over the whole Lago Maggiore area, but additional investigations for a sub-area showed a similar skill to that for the entire region. They found that NORA performs generally better than Eulerian persistence for the lower threshold, but not for the higher threshold. Our performance analysis for discharge forecasts shows that NORA performs better than PERS also for high thresholds, as well as for all catchments on all thresholds over all lead times. Since the events forecast by NORA tend to be persistent by definition, the fact that it also performs better than PERS for short lead times is a valuable finding (Panziera et al., 2011). Moreover, we do not integrate our analysis over the whole Lago Maggiore area, but we analyse the performance of NORA and the other forecasting chains for sub-areas. Thus the variability of precipitation over space and time plays a much greater role in our analysis than in that of Panziera et al. (2011). The good performance of NORA compared to PERS for the discharge forecasts can therefore be explained by the way NORA takes into account the evolution of rainfall (growth and dissipation), whereas PERS keeps the last radar image frozen, and also by the fact that NORA is an ensemble approach and thus takes into account the uncertainty in the location, time and intensity of precipitation. Also the forecast chain using REAL

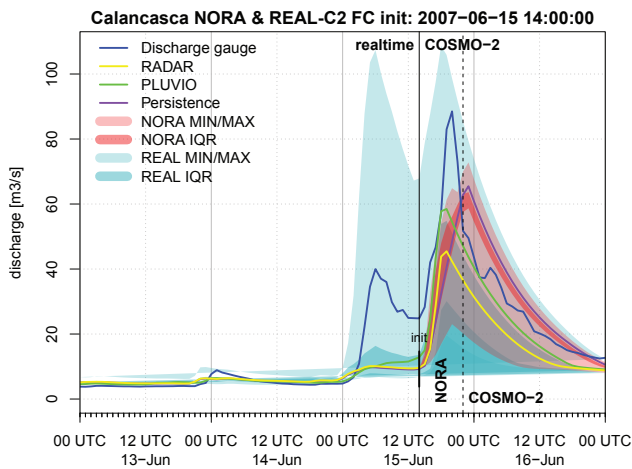


Fig. 8. Forecast simulation for the Calancasca initialised on 15 June at 14:00. For a description, see Fig. 7.

during the nowcast part performs better than PERS. As the spread already develops during the nowcast period the advantage of the ensemble approach comes into effect already at the very start of the forecast period.

Thus, despite the difficulties involved with weather radar estimates in an alpine region, producing these computationally expensive radar-based ensemble forecasts pays off, as the skill of the hydrological forecast is improved already from the start of the forecast period and stays higher also for longer lead times.

4.1 Effect of ensemble forcing: NORA vs. RAD-C2

Panziera et al. (2011) also compared the performance of NORA with the performance of COSMO-2 for the same rainfall thresholds. For light rainfall (threshold $> 0.5 \text{ mm h}^{-1}$), they found NORA to be better than COSMO-2 for 1–2 h lead times, and for the higher threshold (3 mm h^{-1}) NORA outperformed COSMO-2 up to a lead time of 3–4 h. In the corresponding experiment in our study, we compared NORA with RAD-C2, and found that for thresholds up to q80, NORA generally performs better than RAD-C2 for all lead times, except for Calancasca on lead times 4 to 5 h. For the Ticino and Calancasca catchments, the 95 % interval of the bootstrapped BSS values of NORA and RAD-C2 overlap quite a lot (Fig. 5a), but a Student's *t* test on a 5 % significance level showed that BSS values of RAD-C2 and NORA are all different apart from Ticino q70 with lead times 4 h and 5 h, q90 lead time 7 h and Calancasca q60 lead time 3 h. The advantage of NORA over RAD-C2 up to q80 is, however, clear for the Verzasca Basin. For the highest quantiles (q90 and q95), the results differ between the catchments. However, for the Calancasca NORA significantly outperforms RAD-C2 from 4 h lead time onwards. For Verzasca, on the other hand, NORA performs better than RAD-C2 up to 5 to 7 h. Forecasts for Ticino basically show no skill on the highest

quantile, except NORA on q90, but the BSS values are very small, probably because of the general overforecasting on these high quantiles as the catchment is influenced heavily by water management. It should be noted that the uncertainty of the results for forecast performances is larger the higher the threshold (Fig. 5b), due to the fact that fewer data points lie over the high thresholds. However, in most cases NORA shows higher scores than RAD-C2, which is indicative of the added value in using an ensemble forcing for the hydrological modelling.

4.2 Effect of using an ensemble of initial conditions: REAL-C2 vs. RAD-C2

The effect of using an ensemble of initial conditions is shown by the comparison of REAL-C2 and RAD-C2. The difference in forecast performance is a function of the model states after the nowcast period alone, as both forecast chains are forced with the same data during the forecast period. The REAL-C2 forecasting chain performs significantly better than RAD-C2. The BSS values are higher for all thresholds and lead times in all catchments. Furthermore, the 95 % confidence interval of the bootstrapped BSS values is mostly narrower for REAL-C2 and does mostly not overlap with the 95 % confidence interval of the bootstrapped BSS values of RAD-C2. So using an ensemble of initial conditions significantly improved the forecast skill.

4.3 Radar-based ensemble forecasts: REAL-C2 vs. NORA

REAL-C2 forecasts perform better than NORA forecasts in all three catchments. This suggests that an ensemble of initial conditions is more valuable than an ensemble forecast forcing alone. So, for regions where REAL can be produced, that is, in regions where the space-time variance and the autocovariance of radar errors are known, REAL would be preferred over NORA. REAL also has the advantage that it can be produced continuously and that it is not restricted to orographic precipitation. Nevertheless, NORA can offer a useful method to predict near-future discharge in regions where these requirements are not fulfilled, in situations where orographic precipitation (or any other repetitive weather situation) plays a major role in flash-flood triggering and a continuous series of weather radar data is available.

However, the fact that REAL is not only for orographic precipitation is important as an analysis of all exceedances of the q95 threshold from mid June 2007, when the first NORA forecast was made, to December 2010 showed, that a significant part of all threshold exceedances were not covered by a NORA forecast. For Verzasca, 31 % of the q95 threshold exceedances lie outside the hours forecast by NORA, for Calancasca 46 %, and for Ticino 42 %. One reason for this is that the NORA archive contains only situations with orographic precipitation that can be detected by predictors, and

excludes local convective events for computational reasons and because spatially and temporally limited events usually do not result in critical situations (Panziera et al., 2011). This may be correct if the whole Lago Maggiore region is considered, but local convective storms can indeed result in extreme discharge events if they remain stationary over a specific catchment.

The advantage of REAL-C2 over NORA is also supported by the ROC areas, which are a measure of the potential skill of the forecasts if the model is correctly calibrated. For the Ticino and Calancasca catchments, the ROC areas for REAL-C2 are always larger than those for NORA. This means that, even if the system has been correctly calibrated with radar data, REAL-C2 would outperform NORA for the current set-up of our study. For the Verzasca Catchment, REAL-C2 seems to perform better than NORA only on short lead times.

4.3.1 Ensemble spread

Regarding the spread, the two ensembles behave as expected over the eight hours analysed. NORA forecasts show an increasing spread over lead time. Even though the forcing analogues of the NORA ensemble are very similar, the evolution following this initial time step can be very different, and the possibility of divergence between the individual members increases with each time step as long as there is still precipitation. A NORA forecast also always starts with a single initial state at time t_0 (Fig. 4). REAL-C2, on the other hand, is initialised four days prior to the initialisation of NORA, by which time it has already built up some spread. Thus the influence of the initial state is minor after these four days. At time t_0 the REAL nowcast is connected with the latest available COSMO-2 forecast. This means that the deterministic COSMO-2 is started with 25 different initial conditions. As the REAL ensemble will have already developed its spread prior to the connection, the change in spread over the following eight hours is not as big as for the NORA ensemble, which starts from one single initial state. As soon COSMO-2 stops adding more precipitation the ensemble members converge.

The Verzasca is noticeably the only catchment where the spread of the REAL-C2 ensemble decreases with lead time, possibly due to the nature of the events included in the study period. NORA is only produced if the atmospheric conditions favour orographic precipitation, which means in the Lago Maggiore region, that the winds are blowing from the southwest or south (Panziera et al., 2011). Thus storms usually move roughly from southwest to northeast, and therefore arrive and leave the Verzasca Basin earlier than the Ticino and Calancasca Basin. This also affects the timing of the discharge peaks of the major events within the study period, and the Verzasca River usually peaks at least one hour earlier than the Calancasca River for the events analysed. The Ticino River also peaks after the Verzasca River, but here the

reason is most likely that the Ticino catchment is one order of magnitude bigger than the Verzasca Catchment, and thus reacts more slowly.

The single event in the Calancasca River presented in Figs. 7 and 8 shows that the relatively old COSMO-2 forecast available prior to the event, on 14 June 2007 at 23:00, dampens the performance of REAL-C2. COSMO-2 forecasts only little rain for the first about 15 h of our forecast, so that the spread of REAL-C2 does not grow much over the first hours. In such situations NORA can help detect critical situations earlier. However, the comparison with the forecast initialised during the ongoing event suggests that the potential of NORA forecasts mainly lies in the early detection of a coming event rather than in forecasting the magnitude of an event, but more individual events need to be analysed, to be able to draw a general conclusion.

4.4 The reference forecast: PLU-C2

The pluviometer-based forecasts PLU-C2 perform well compared to the other forecasting chains, and in some cases even outperform REAL-C2 (Calancasca q70 and q90 at long lead times, Verzasca q80 at short lead times) (Fig. 5). One reason for this relatively good performance of the deterministic PLU-C2 is that the hydrological model was calibrated with rain-gauge data, and this calibration is also the basis for all the model chains based on weather radar data. Furthermore, a bias correction factor derived during calibration is applied to all interpolated rain-gauge data. The weather radar data are, however, due to the lack of a homogenous time series long enough to perform a calibration, used without such a correction factor. Thus PLU provides the better initial conditions for the COSMO-2 forced forecasts.

Although the PLU-C2 forecasting chain performs generally relatively well, there are quite some differences between the individual catchments. On the highest quantiles q90 and q95, PLU-C2 has no skill in the Ticino catchment, whereas for the Verzasca and Calancasca catchments it is still skilful. This difference for the Ticino catchment can be explained by looking at the bias of PLU-C2 for the Ticino catchment. The PLU-C2 forecasts for Ticino are very positively biased on the highest quantiles. The other forecasting chains also show a positive bias, but not that extreme, as is also indicated by the high FAR combined with still relatively high POD values for high threshold quantiles. Thus extreme events are overforecasted for the Ticino River, possibly due to the influence of several storage lakes for hydropower production. The precipitation that actually falls in the catchment is not then recorded at the catchment outlet at the estimated time, but is stored in the lakes.

The interpolated precipitation maps are, however, generally good as PLU-C2 performed well in the Verzasca Catchment and especially well in the Calancasca Catchment, where the PLU-C2 forecasts are mostly unbiased despite the lack of a rain-gauge in the catchment (Fig. 1). However, the

good performance of PLU-C2 is mostly connected to the fact that PREVAH was calibrated using interpolated rain-gauge data, including a bias correction factor.

5 Conclusions

Our study explored the potential of radar-based ensemble forecasts for flash-flood early warning by comparing two novel radar-based ensemble forecast chains to deterministic forecast products in three catchments of the southern Swiss Alps using the hydrological model system PREVAH. Special emphasis was placed on the added value of the purely radar-based NORA forecasting system. NORA is an analogue-based ensemble forecast for orographic precipitation, consisting of 12 members, initialised with the initial conditions derived from a four-day nowcast with deterministic radar QPE. The second ensemble forecasting system evaluated in our study is REAL-C2, where COSMO-2 is initialised with 25 different initial conditions derived from a four-day nowcast with the radar ensemble REAL. Additionally, three deterministic forecasting chains were analysed. One is the persistence of the radar QPE at t_0 (PERS), while the other two are COSMO-2 forecasts initialised with initial conditions derived from a four-day deterministic nowcast with radar QPEs (RAD-C2) and interpolated rain-gauge data (PLU-C2). We analysed the performance of these five flash-flood forecasting systems for all hours between June 2007 and December 2010 for which NORA forecasts were issued, when triggered by orographic precipitation.

We found a clear preference for the ensemble approach. NORA generally outperformed RAD-C2 for thresholds up to q_{80} . This shows that a radar-based ensemble forcing of the hydrological forecast is superior to a deterministic forcing as provided by COSMO-2. Moreover, the better performance of REAL-C2 over RAD-C2 shows the positive effect of working with an ensemble of initial conditions. Furthermore, REAL-C2 performed better than NORA. This comparison leads to the conclusion that the positive effect of an ensemble of initial conditions is bigger than the positive effect of using a ensemble forecast forcing alone.

A follow-up study may also analyse NORA forecasts with a temporal resolution smaller than one hour. This would potentially further enhance the performance in forecasting the timing and magnitude of flash-flood events, and could be beneficial especially for small catchments with very short response time. For computational reasons a simple rainfall-runoff model as proposed by Kirchner (2009) may be considered for this purpose. Future investigations may also use NORA forecasts to derive initial conditions for a subsequent initialisation of NWP forecasts, as in REAL-C2. See the example in Figs. 7 and 8, where COSMO-2 is connected to NORA after eight hours. The ideal time for connecting NORA to COSMO-2 still needs to be decided. According to the results for the Calancasca and Verzasca catchments,

the ideal time for switching from NORA to an NWP forecast would probably be after 4 to 5 h. This is also in agreement with Panziera et al. (2011) who found that after 4 to 5 h COSMO-2 precipitation forecasts generally perform better than NORA. A connection between REAL and NORA could thus be considered for future work. This would result in an ensemble of 300 members, which would most probably show a very large spread. Thus, to be useful for decision making, some sort of pre-selection of behavioural members would be required. First tests using the Series Distance method (Ehret and Zehe, 2011) to rank REAL members encourage further investigations in this direction. An analysis of this approach would, however, be beyond the scope of the study presented here.

Our study also showed that a well-maintained rain-gauge network is very useful. Nowcasts forced by rain-gauge data provide good initial conditions for subsequent forecasts. Also the rain-gauge data are needed to investigate the space-time variance and auto-covariance of radar errors, which is a prerequisite for producing the radar ensemble REAL. For regions covered by a rain-gauge network the application of a rain-gauged precipitation ensemble generator as proposed in Rakovec et al. (2012) or Moulin et al. (2009) would be a further option to account for the uncertainty in the meteorological input to the hydrological model. Such a rain-gauge-based ensemble could be used, in the same way as REAL was used in our study, to derive an ensemble of initial conditions for a subsequent hydrological forecast forced by NWP data. However, the presented study focused on the use of radar-based ensemble forecasts which are not only restricted to regions covered by a good rain-gauge network. In this respect the calibration of the hydrological model with weather radar data would be most desirable in order to further improve the forecast performance. However, this would require a long continuous series of weather radar data.

Generally we can conclude that, if the data required to produce REAL are available, REAL-C2 is the preferred forecasting chain because it performs better than NORA and is not restricted to events originating from orographic precipitation. However, for regions where REAL cannot be produced, NORA might be an option to forecast events triggered by orographic rainfall.

Acknowledgements. We are grateful to MeteoSwiss for permission to use data from their ground-based and weather radar networks, and to the Swiss Federal Office for Environment for providing us with runoff data from their networks. The authors were fully or partly financed through the EU FP7 Project IMPRINTS (Grant agreement no.: 226555/FP7-843 ENV-2008-1-226555). Special thanks to Felix Fundel for his support with statistics and programming and to Silvia Dingwall for language editing. We thank two independent reviewers for their valuable comments on an earlier version of this paper.

Edited by: R. Uijlenhoet

References

- Addor, N., Jaun, S., Fundel, F., and Zappa, M.: An operational hydrological ensemble prediction system for the city of Zurich (Switzerland): skill, case studies and scenarios, *Hydrol. Earth Syst. Sci.*, 15, 2327–2347, doi:10.5194/hess-15-2327-2011, 2011.
- AghaKouchak, A., Nakhjiri, N., and Habib, E.: An educational model for ensemble streamflow simulation and uncertainty analysis, *Hydrol. Earth Syst. Sci.*, 17, 445–452, doi:10.5194/hess-17-445-2013, 2013.
- Ahrens, B. and Jaun, S.: On evaluation of ensemble precipitation forecasts with observation-based ensembles, *Adv. Geosci.*, 10, 139–144, doi:10.5194/adgeo-10-139-2007, 2007.
- Alfieri, L., Thielen, J., and Pappenberger, F.: Ensemble hydro-meteorological simulation for flash flood early detection in southern Switzerland, *J. Hydrol.*, 424, 143–153, doi:10.1016/j.jhydrol.2011.12.038, 2012.
- Ament, F., Weusthoff, T., and Arpagaus, M.: Evaluation of MAP D-PHASE heavy precipitation alerts in Switzerland during summer 2007, *Atmos. Res.*, 100, 178–189, 2011.
- Bartholmes, J. C., Thielen, J., Ramos, M. H., and Gentilini, S.: The european flood alert system EFAS – Part 2: Statistical skill assessment of probabilistic and deterministic operational forecasts, *Hydrol. Earth Syst. Sci.*, 13, 141–153, doi:10.5194/hess-13-141-2009, 2009.
- Berenguer, M., Corral, C., Sanchez-Diezma, R., and Sempere-Torres, D.: Hydrological validation of a radar-based nowcasting technique, *J. Hydrometeorol.*, 6, 532–549, 2005.
- Bowler, N. E., Pierce, C. E., and Seed, A. W.: STEPS: A probabilistic precipitation forecasting scheme which merges an extrapolation nowcast with downscaled NWP, *Q. J. Roy. Meteorol. Soc.*, 132, 2127–2155, 2006.
- Bowler, N. E., Arribas, A., Mylne, K. R., Robertson, K. B., and Beare, S. E.: The MOGREPS short-range ensemble prediction system, *Q. J. Roy. Meteorol. Soc.*, 134, 703–722, doi:10.1002/qj.234, 2008.
- Buizza, R., Hollingsworth, A., Lalaurette, E., and Ghelli, A.: Probabilistic predictions of precipitation using the ECMWF ensemble prediction system, *Weather Forecast.*, 14, 168–189, doi:10.1175/1520-0434(1999)014<0168:ppoput>2.0.co;2, 1999.
- Efron, B.: Jackknife-after-Bootstrap Standard Errors and Influence Functions, *J. Roy. Stat. Soc. B Met.*, 54, 83–127, 1992.
- Ehret, U. and Zehe, E.: Series distance – an intuitive metric to quantify hydrograph similarity in terms of occurrence, amplitude and timing of hydrological events, *Hydrol. Earth Syst. Sci.*, 15, 877–896, doi:10.5194/hess-15-877-2011, 2011.
- Fundel, F. and Zappa, M.: Hydrological ensemble forecasting in mesoscale catchments: Sensitivity to initial conditions and value of reforecasts, *Water Resour. Res.*, 47, W09520, doi:10.1029/2010wr009996, 2011.
- Fundel, F., Walser, A., Liniger, M. A., Frei, C., and Appenzeller, C.: Calibrated Precipitation Forecasts for a Limited Area Ensemble Forecast System Using Reforecasts, *Mon. Weather Rev.*, 138, 176–189, 2010.
- Germann, U. and Zawadzki, I.: Scale-Dependence of the Predictability of Precipitation from Continental Radar Images. Part I: Description of the Methodology, *Mon. Weather Rev.*, 130, 2859–2873, doi:10.1175/1520-0493(2002)130<2859:sdotpo>2.0.co;2, 2002.
- Germann, U. and Zawadzki, I.: Scale Dependence of the Predictability of Precipitation from Continental Radar Images. Part II: Probability Forecasts, *J. Appl. Meteorol.*, 43, 74–89, doi:10.1175/1520-0450(2004)043<0074:sdotpo>2.0.co;2, 2004.
- Germann, U., Galli, G., Boscacci, M., and Bolliger, M.: Radar precipitation measurement in a mountainous region, *Q. J. Roy. Meteorol. Soc.*, 132, 1669–1692, doi:10.1256/qj.05.190, 2006.
- Germann, U., Berenguer, M., Sempere-Torres, D., and Zappa, M.: REAL - Ensemble radar precipitation estimation for hydrology in a mountainous region, *Q. J. Roy. Meteorol. Soc.*, 135, 445–456, doi:10.1002/qj.375, 2009.
- Gurtz, J., Zappa, M., Jasper, K., Lang, H., Verbunt, M., Badoux, A., and Vitvar, T.: A comparative study in modelling runoff and its components in two mountainous catchments, *Hydrol. Process.*, 17, 297–311, doi:10.1002/hyp.1125, 2003.
- Jaun, S. and Ahrens, B.: Evaluation of a probabilistic hydrometeorological forecast system, *Hydrol. Earth Syst. Sci.*, 13, 1031–1043, doi:10.5194/hess-13-1031-2009, 2009.
- Jaun, S., Ahrens, B., Walser, A., Ewen, T., and Schär, C.: A probabilistic view on the August 2005 floods in the upper Rhine catchment, *Nat. Hazards Earth Syst. Sci.*, 8, 281–291, doi:10.5194/nhess-8-281-2008, 2008.
- Kirchner, J. W.: Catchments as simple dynamical systems: Catchment characterization, rainfall-runoff modeling, and doing hydrology backward, *Water Resour. Res.*, 45, W02429, doi:10.1029/2008wr006912, 2009.
- Liechti, K., Zappa, M., Fundel, F., and Germann, U.: Probabilistic evaluation of ensemble discharge nowcasts in two nested Alpine basins prone to flash floods, *Hydrol. Process.*, 27, 5–17, doi:10.1002/hyp.9458, 2013.
- Mandapaka, P. V., Germann, U., Panziera, L., and Hering, A.: Can Lagrangian Extrapolation of Radar Fields be used for Precipitation Nowcasting over Complex Alpine Orography?, *Weather Forecast.*, 27, 28–49, doi:10.1175/waf-d-11-00050.1, 2012.
- Michelson, D. B.: Systematic correction of precipitation gauge observations using analyzed meteorological variables, *J. Hydrol.*, 290, 161–177, 2004.
- Montani, A., Cesari, D., Marsigli, C., and Paccagnella, T.: Seven years of activity in the field of mesoscale ensemble forecasting by the COSMO-LEPS system: main achievements and open challenges, *Tellus A*, 63, 605–624, doi:10.1111/j.1600-0870.2010.00499.x, 2011.
- Morin, E., Jacoby, Y., Navon, S., and Bet-Halachmi, E.: Towards flash-flood prediction in the dry Dead Sea region utilizing radar rainfall information, *Adv. Water Resour.*, 32, 1066–1076, 2009.
- Moulin, L., Gaume, E., and Obled, C.: Uncertainties on mean areal precipitation: assessment and impact on streamflow simulations, *Hydrol. Earth Syst. Sci.*, 13, 99–114, doi:10.5194/hess-13-99-2009, 2009.
- Panziera, L. and Germann, U.: The relation between airflow and orographic precipitation on the southern side of the Alps as revealed by weather radar, *Q. J. Roy. Meteorol. Soc.*, 136, 222–238, doi:10.1002/qj.544, 2010.
- Panziera, L., Germann, U., Gabella, M., and Mandapaka, P. V.: NORA–Nowcasting of Orographic Rainfall by means of Analogues, *Q. J. Roy. Meteorol. Soc.*, 137, 2106–2123, doi:10.1002/qj.878, 2011.
- Price, D., Hudson, K., Boyce, G., Schellekens, J., Moore, R. J., Clark, P., Harrison, T., Connolly, E., and Pilling, C.: Operational

- use of a grid-based model for flood forecasting, *P. I. Civil Eng.-Wat. M.*, 165, 65–77, doi:10.1680/wama.2012.165.2.65, 2012a.
- Price, D., Pilling, C., Robbins, G., Lane, A., Boyce, G., Fenwick, K., Moore, R. J., Coles, J., Harrison, T., and Van Dijk, M.: Representing the spatial variability of rainfall for input to the G2G distributed flood forecasting model: operational experience from the Flood Forecasting Centre, in: *Weather Radar and Hydrology*, IAHS Publication, 532–537, 2012b.
- Rakovec, O., Hazenberg, P., Torfs, P. J. J. F., Weerts, A. H., and Uijlenhoet, R.: Generating spatial precipitation ensembles: impact of temporal correlation structure, *Hydrol. Earth Syst. Sci.*, 16, 3419–3434, doi:10.5194/hess-16-3419-2012, 2012.
- Ranzi, R., Zappa, M., and Bacchi, B.: Hydrological aspects of the Mesoscale Alpine Programme: Findings from field experiments and simulations, *Q. J. Roy. Meteorol. Soc.*, 133, 867–880, doi:10.1002/qj.68, 2007.
- Rossa, A. M., Laudanna Del Guerra, F., Borga, M., Zanon, F., Settin, T., and Leuenberger, D.: Radar-driven high-resolution hydro-meteorological forecasts of the 26 September 2007 Venice flash flood, *J. Hydrol.*, 394, 230–244, 2010.
- Rossa, A., Liechti, K., Zappa, M., Bruen, M., Germann, U., Haase, G., Keil, C., and Krahe, P.: The COST 731 Action: A review on uncertainty propagation in advanced hydro-meteorological forecast systems, *Atmos. Res.*, 100, 150–167, doi:10.1016/j.atmosres.2010.11.016, 2011.
- Rotach, M. W., Ambrosetti, P., Ament, F., Appenzeller, C., Arpagaus, M., Bauer, H.-S., Behrendt, A., Bouttier, F., Buzzi, A., Corazza, M., Davolio, S., Denhard, M., Dorninger, M., Fontannaz, L., Frick, J., Fundel, F., Germann, U., Gorgas, T., Hegg, C., Hering, A., Keil, C., Liniger, M. A., Marsigli, C., McTaggart-Cowan, R., Montaini, A., Mylne, K., Ranzi, R., Richard, E., Rossa, A., Santos-Muñoz, D., Schär, C., Seity, Y., Staudinger, M., Stoll, M., Volkert, H., Walser, A., Wang, Y., Werhahn, J., Wulfmeyer, V., and Zappa, M.: MAP D-PHASE: Real-Time Demonstration of Weather Forecast Quality in the Alpine Region, *B. Am. Meteorol. Soc.*, 90, 1321–1336, doi:10.1175/2009BAMS2776.1, 2009.
- Schellekens, J., Weerts, A. H., Moore, R. J., Pierce, C. E., and Hildon, S.: The use of MOGREPS ensemble rainfall forecasts in operational flood forecasting systems across England and Wales, *Adv. Geosci.*, 29, 77–84, doi:10.5194/adgeo-29-77-2011, 2011.
- Seed, A. W.: A Dynamic and Spatial Scaling Approach to Advection Forecasting, *J. Appl. Meteorol.*, 42, 381–388, 2003.
- Sevruk, B.: Adjustment of tipping-bucket precipitation gauge measurements, *Atmos. Res.*, 42, 237–246, 1996.
- Szturc, J., Ośródk, K., Jurczyk, A., and Jelonek, L.: Concept of dealing with uncertainty in radar-based data for hydrological purpose, *Nat. Hazards Earth Syst. Sci.*, 8, 267–279, doi:10.5194/nhess-8-267-2008, 2008.
- Tobin, C., Nicotina, L., Parlange, M. B., Berne, A., and Rinaldo, A.: Improved interpolation of meteorological forcings for hydrologic applications in a Swiss Alpine region, *J. Hydrol.*, 401, 77–89, 2011.
- Velasco-Forero, C. A., Sempere-Torres, D., Cassiraga, E. F., and Gómez-Hernández, J.: A non-parametric automatic blending methodology to estimate rainfall fields from rain gauge and radar data, *Adv. Water Resour.*, 32, 986–1002, 2009.
- Villarini, G., Mandapaka, P. V., Krajewski, W. F., and Moore, R. J.: Rainfall and sampling uncertainties: A rain gauge perspective, *J. Geophys. Res.-Atmos.*, 113, D11102, doi:10.1029/2007jd009214, 2008.
- Viviroli, D., Zappa, M., Gurtz, J., and Weingartner, R.: An introduction to the hydrological modelling system PREVAH and its pre- and post-processing-tools, *Environ. Modell. Softw.*, 24, 1209–1222, doi:10.1016/j.envsoft.2009.04.001, 2009a.
- Viviroli, D., Zappa, M., Schwanbeck, J., Gurtz, J., and Weingartner, R.: Continuous simulation for flood estimation in ungauged mesoscale catchments of Switzerland – Part I: Modelling framework and calibration results, *J. Hydrol.*, 377, 191–207, 2009b.
- Werner, M. and Cranston, M.: Understanding the Value of Radar Rainfall Nowcasts in Flood Forecasting and Warning in Flashy Catchments, *Meteorol. Appl.*, 16, 41–55, 2009.
- Weusthoff, T., Ament, F., Arpagaus, M., and Rotach, M. W.: Assessing the Benefits of Convection-Permitting Models by Neighborhood Verification: Examples from MAP D-PHASE, *Mon. Weather Rev.*, 138, 3418–3433, doi:10.1175/2010mwr3380.1, 2010.
- Wilks, D. S.: *Statistical methods in the atmospheric sciences*, 2nd Edn., Elsevier, Amsterdam, 627 pp., 2006.
- Wöhling, Th., Lennartz, F., and Zappa, M.: Technical Note: Updating procedure for flood forecasting with conceptual HBV-type models, *Hydrol. Earth Syst. Sci.*, 10, 783–788, doi:10.5194/hess-10-783-2006, 2006.
- Zappa, M. and Kan, C.: Extreme heat and runoff extremes in the Swiss Alps, *Nat. Hazards Earth Syst. Sci.*, 7, 375–389, doi:10.5194/nhess-7-375-2007, 2007.
- Zappa, M., Rotach, M. W., Arpagaus, M., Dorninger, M., Hegg, C., Montani, A., Ranzi, R., Ament, F., Germann, U., Grossi, G., Jaun, S., Rossa, A., Vogt, S., Walser, A., Wehrhan, J., and Wunram, C.: MAP D-PHASE: real-time demonstration of hydrological ensemble prediction systems, *Atmos. Sci. Lett.*, 9, 80–87, doi:10.1002/asl.183, 2008.
- Zappa, M., Jaun, S., Germann, U., Walser, A., and Fundel, F.: Superposition of three sources of uncertainties in operational flood forecasting chains, *Atmos. Res.*, 100, 246–262, doi:10.1016/j.atmosres.2010.12.005, 2011.